Journal of Materials Chemistry

Cite this: J. Mater. Chem., 2012, 22, 4371

www.rsc.org/materials

PAPER

Characterisation of a dipolar chromophore with third-harmonic generation applications in the near-IR†

Yulia A. Getmanenko,[a] Joel M. Hales,[b] Mihaela Balu,[b] Jie Fu,[b] Egbert Zojer,[ac] Ohyun Kwon,[a] Jeffrey Mendez,[d] S. Thayumanavan,[d] Gregory Walker,[e] Qing Zhang,[a] Scott D. Bunge,[f] Jean-Luc Brédas,[a] David J. Hagan,[b] Eric W. Van Stryland,[b] Stephen Barlow[ae] and Seth R. Marder[ade]

Received 1st November 2011, Accepted 1st December 2011
DOI: 10.1039/c2jm15599k

E-2-Tricyanovinyl-3-*n*-hexyl-5-[4-{bis(4-*n*-butylphenyl)amino}-2-methoxystyryl]-thiophene, **1**, has previously been used to demonstrate applications relying on frequency tripling of 1.55 μm light. Here we report the synthesis and chemical characterisation of **1**, along with quantum-chemical calculations and additional experimental investigations of its third-order nonlinear properties that give more insight into its frequency tripling properties. Although **1** can be processed into amorphous films, crystals can also be grown by slow evaporation of solutions; the crystal structure determined by X-ray diffraction shows evidence of significant contributions from zwitterionic resonance forms to the ground-state structure, and reveals centrosymmetric packing exhibiting π–π and C–H···N≡C interactions. Both solutions and films of **1** exhibit near-infrared two-photon absorption into the low-lying one-photon-allowed state with a peak two-photon cross-section of *ca.* 290 GM (measured using the white-light continuum method with a pump wavelength of 1800 nm) at a transition energy equivalent to degenerate two-photon absorption at *ca.* 1360 nm; two related chromophores are also found to show comparable near-IR two-photon cross-sections. Closed-aperture Z-scan measurements and quantum-chemical calculations indicate that the nonlinear refractive index and third-harmonic generation properties of **1** are strongly dependent on frequency in the telecommunications range, due the aforementioned two-photon resonance.

Introduction

Organic materials with large third-order optical susceptibilities, $\chi^{(3)}$,[1] can be exploited for a wide variety of applications including all-optical switching (AOS)[2–5] and correlation for laser diagnostics and image recognition.[6–8] We have previously reported a range of hydroxy-functionalised chromophores, including **I** (Fig. 1), in which dicyanovinyl or tricyanovinyl acceptors are attached to the 5-position of thiophenes linked by a vinylene bridge in the 2 position to triarylamine donors.[9] Our interest was originally in the use of these compounds as thermally and photochemically stable chromophores with large second-order polarisabilities, β. Specifically we were concerned with their use as electric-field-poled materials for electrooptic switching of light in the telecommunications band (1.3–1.55 μm), when covalently linking them to host polymers *via* the hydroxy-functionality.[10–12] Diarylamino donors were chosen due to their superior stability compared to the more widely used dialkylamino groups;[13–15] the vinylene-thienylene portions of the bridges were used as compromises between the low stability of polyene bridges and

[a]*School of Chemistry and Biochemistry and Center for Organic Photonics and Electronics, Georgia Institute of Technology, Atlanta, GA, 30332-0400, USA*
[b]*CREOL & FPCE, The College of Optics and Photonics and Department of Physics, University of Central Florida, Orlando, FL, 32816-2700*
[c]*Institute of Solid State Physics, Graz University of Technology, 8010 Graz, Austria*
[d]*Beckman Institute, California Institute of Technology, Pasadena, CA, 91125, USA*
[e]*Department of Chemistry, University of Arizona, Tucson, AZ, 85721, USA*
[f]*Department of Chemistry and Biochemistry, Kent State University, Kent, OH, 44242-0001, USA*

† Electronic supplementary information (ESI) available: DSC and TGA data for **1** and 2PA spectra for **2** and **3**, and calculated dispersions of γ for **1**. CCDC reference number 851132 (**1**). For ESI and crystallographic data in CIF or other electronic format see DOI: 10.1039/c2jm15599k

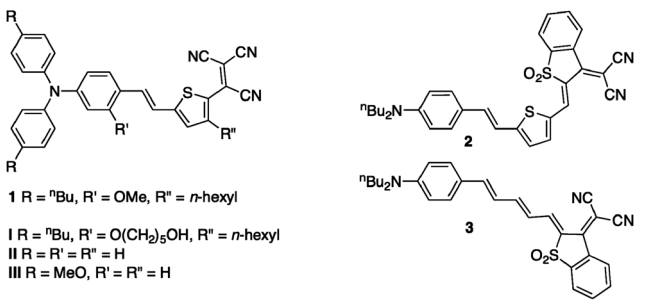

Fig. 1 Structure of chromophores **1–3** and some previously studied related chromophores **I–III**.

the tendency of phenylene-based bridges to discourage significant contributions from zwitterionic resonance structures and, thus, to afford lower nonlinearities;[14,16–20] and the alkyl chains were introduced to promote solution processability. Although designed for second-order nonlinear applications, moderate to large third-order polarisabilities, γ, can also be obtained in donor–acceptor chromophores with correctly balanced donor and acceptor strengths,[21–23] and the linear absorption spectrum of **I** appeared promising for applications involving frequency tripling of 1.55 μm light due to a minimum in the absorption spectrum around the third harmonic (517 nm) and good transparency at the fundamental wavelength. Using an analogue of **I** without hydroxy functionalisation, **1**, we demonstrated third-harmonic generation (THG) applications at this wavelength including an optical autocorrelator for time-domain operation,[24] ultrafast pulse diagnostics based on frequency-resolved optical gating,[25] and imaging through scattering media.[26–28] However, the synthesis and chemical characterisation of **1** were not described in that work; here we report on these aspects of **1**, along with its crystal structure and with additional experimental and quantum-chemical studies of its third-order nonlinear optical properties. In particular, since the linear absorption spectrum of **1** exhibits an absorption maximum of *ca.* 650 nm and since one-photon states in dipolar systems are also two-photon allowed, with the two-photon absorption (2PA) cross-sections (δ) in an essential-state picture dominated by the same terms that determine β, we investigated the possibility of 2PA in the telecommunications wavelength range. This is of interest for applications including optical pulse suppression,[29,30] all-optical beam stabilisation, dynamic-range compression, and photorefractivity.[31,32] Moreover, we compared the 2PA spectra with those of two previously reported dipolar high-β chromophores, **2**[20,33] and **3**,[33,34] that exhibit similar linear absorption maxima; **3** has previously been used for the 2PA-induced sensitisation of photorefractive composites at 1.55 μm.[31,32]

Results

Synthesis and characterisation

Chromophore **1** was prepared in a similar fashion to that described for its hydroxy-functionalised analogue, **I**.[9] The diarylaminobenzaldehyde **5** was obtained as shown in Scheme 2 by formylation of the known triarylamine **4**[9] using standard Vilsmeier–Haack conditions. The Wittig reaction between **5** and the phosphonium salt **6**[9] gave intermediate **7**. Compounds **I** and **II** and related species were previously obtained by lithiation of the relevant precursors in THF, followed by treatment with tetracyanoethylene (TCNE).[9,35] However, thiophene derivatives are also known to react directly with TCNE in DMF, without a lithiation step, to give tricyanovinyl-substituted species;[36,37] indeed, chromophore **III**, which is structurally similar to **1**, has been obtained in this way.[38] This method was successfully used in the preparation of **1**; since the electron-rich nature of **7** renders it rather unstable, it was converted to **1** immediately subsequent to purification by column chromatography (Scheme 1). Although the Wittig reaction is anticipated to give a mixture of *E* and *Z* isomers of **7**, only a single isomer of **1**, shown by X-ray crystallography (*vide infra*) to be the *E* isomer, was obtained; as in our previous work,[9] introduction of the tricyanovinyl acceptor facilitates isomerisation, presumably through reduction of the barrier to rotation about the C=C bond due to increased contributions from zwitterionic resonance forms.

The phosphonium salt **6** was prepared from 4-*n*-hexylthiophen-2-yl methanol, **12**, as previously described.[9] Compound **12** can either be obtained in several steps from 4-bromothiophene-2-carboxaldehyde, as previously described,[9] or in several high-yielding steps from a more inexpensive starting material, 3-bromothiophene. This new route is shown in Scheme 2; 3-bromothiophene was selectively lithiated and silylated using lithium diisopropylamide and trimethylchlorosilane to give 2-trimethylsilyl-3-bromothiophene, **8**, in high yield. Kumada coupling of **8** with *n*-hexylmagnesium bromide in THF afforded 2-(trimethylsilyl)-3-(*n*-hexyl)thiophene, **9**. Compound **9** was formylated by treatment with *n*-butyllithium, followed by trapping with DMF and acidic work up; the resulting aldehyde, **10**, was reduced to the corresponding alcohol, **11**, using sodium borohydride in ethanol. The reaction of tetra(*n*-butyl)ammonium fluoride with **11** to remove the trimethylsilyl group was sluggish; however, after two days of stirring, the intermediate **8** was obtained in 77% yield.

Thermal characterisation

The thermal stability of compound **1** was investigated using thermogravimetric analysis; at a heating rate of 5 °C min^{-1} the onset of weight loss occurred at *ca.* 270 °C, close to the 295 °C decomposition temperature previously reported for the related chromophore, **III** (Fig. 1).[38,39] Differential scanning calorimetry was used to investigate the phase behavior of **1**; heating of a crystalline sample (10 °C min^{-1}) revealed a melting point of 103 °C. However, no recrystallisation was observed on cooling at the same rate and a second heating (5 °C min^{-1}) revealed a glass transition at *ca.* 34 °C. The low melting point of **1** and its reluctance to crystallise are presumably related to the long-chain alkyl substituents and facilitate melt-processing of the material into amorphous films at high chromophore densities. Indeed, melt-processed films of **1** and polystyrene in a 1: 4 weight ratio, which we have used in our previously published studies,[24–26] have been shown to be amorphous and of good optical quality.

Electrochemistry

Cyclic voltammetry (Fig. 2, Table 1) shows that **1** exhibits two successive reversible molecular reductions, as is typical for tricyanovinyl-substituted chromophores.[40] Indeed the half-wave potentials are very similar to those reported for **III** in the same solvent and electrolyte,[38] consistent with the 4-[bis(4-*n*-butylphenyl)amino]-2-methoxyphenyl group of **1** acting as a π donor of comparable strength to the 4-[bis(4-alkoxyphenyl)amino] phenyl group of **III**. The oxidation potential is also similar to that of a previously reported donor–acceptor dye containing the same donor.[41,42] The redox potentials for **2** and **3** are rather similar to those for **1**; compound **2** is both more easily oxidised and reduced than **3**, presumably due to weaker donor–acceptor coupling (*i.e.*, less significant contributions from the zwitterionic resonance structure) through the thiophene-containing bridge of **2** than through the polyene bridge of **3**.

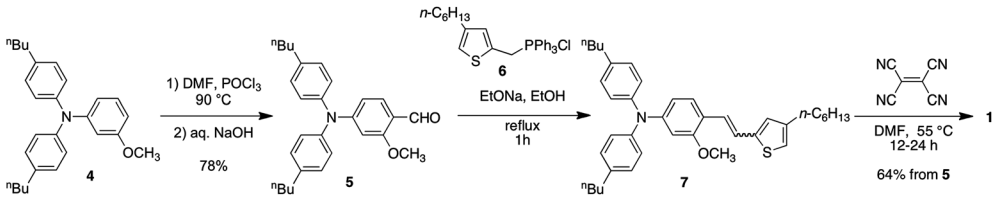

Scheme 1 Synthesis of chromophore **1**.

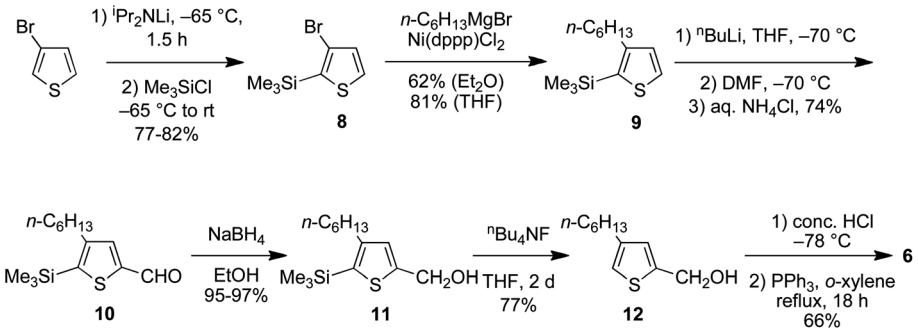

Scheme 2 Alternative synthesis of the precursor to phosphonium salt **6**.

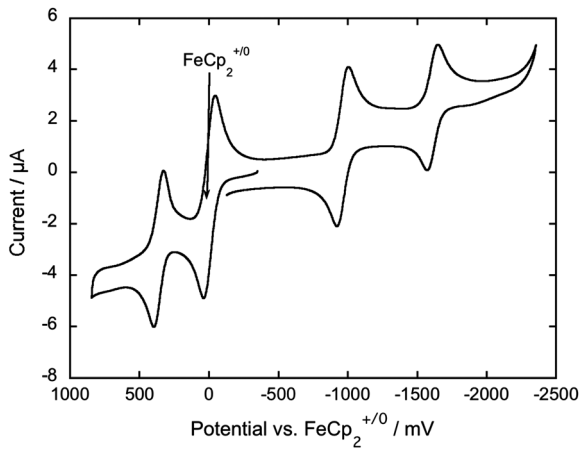

Fig. 2 Cyclic voltammogram at 50 mV s^{-1} of **1** in CH_2Cl_2/0.1 M $^nBu_4NPF_6$ containing ferrocene as an internal reference.

Table 1 Electrochemical potentials (V *vs.* $FeCp_2^{+/0}$) in dichloromethane/0.1 M $^nBu_4NPF_6$ for dipolar chromophores **1–3**

Compound	$E_{1/2}^{+/0}$	$E_{1/2}^{0/-}$	$E_{1/2}^{-/2-}$
1	+0.36	–0.96	–1.61
2	+0.28	–0.90[a]	—
3[43]	+0.37[a]	–0.93[a]	—

[a] EC-type process.

Crystal structure

Slow evaporation of ethyl acetate / hexanes solution of **1** produced crystals suitable for single-crystal X-ray structure determination. As is typical for chromophores with large dipole moments, crystals of **1** were found to belong to a centrosymmetric space group (*C*2/*c*, one molecule in the asymmetric unit and, therefore, four in the unit cell), ruling out bulk second-order nonlinear optical effects. Since many organic compounds, including some examples of donor–acceptor second-order chromophores,[43] exhibit polymorphism, we employed polymer-induced heteronucleation[44,45] to search for alternative (potentially non-centric) crystal forms of **1**. Acetone solutions of **1** were evaporated in the presence of three polymer libraries; however, powder X-ray diffraction patterns of the crystalline materials obtained in each case were consistent with the structure obtained in the single-crystal study.

The structure adopted by the molecules in the crystal is shown in Fig. 3. The π-system is approximately planar, but there is some twisting around the vinylene bridge (angles of *ca.* 6 and 16° between arylene and vinylene planes and between thiophene and vinylene planes, respectively) and in the donor group (angle of 7° between the plane formed by the amino nitrogen atom and its directly attached carbon atoms and that of the methoxy-substituted phenylene group). Due to the possibility of rotation about arene–vinylene (i and i′, Fig. 4a), thiophene-vinylene (ii, ii′), and thiophene-tricyanovinylene (iii, iii′) bonds, several conformations are, in principle, to be anticipated. In the conformation found in the crystal structure, the orientations of the vinylene and tricyanovinylene groups are consistent with expectations from intramolecular steric considerations (*i.e.*, are approximated by ii and iii in Fig. 4a), while the vinylene group is oriented towards the methoxy group of the aryl ring (i′), which is presumably the less favourable orientation from a steric point of view.

Several geometric features of the structure are consistent with zwitterionic resonance structures (Fig. 4b) making a contribution to the ground-state structure of the chromophore. As noted above, the plane formed by the amine nitrogen and its directly attached carbon atoms is close to coplanar with the bridging arylene group (7° between planes), while forming much larger

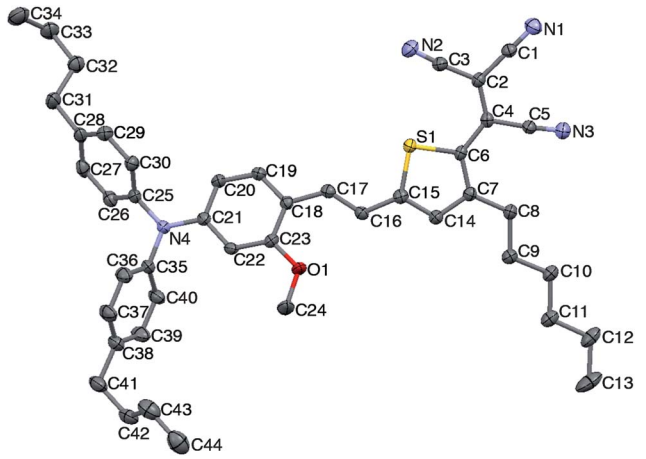

Fig. 3 View of the molecular structure of chromophore **1** in its single-crystal X-ray structure.

angles (59 and 64°) with the planes of the terminal aryl groups (Ar), consistent with the amine acting as a π-donor primarily to the bridging groups. However, it should be noted that, although all three angles in triarylamines are often comparable, both in simple compounds[46] and other triarylamine-based extended π-systems without strong π-acceptors,[47,48] they can show similar patterns of interplanar angles at the amine to that found in **1**,[46] presumably due to crystal-packing effects. More conclusive evidence of the role of the zwitterionic resonance forms comes from bond lengths: the N–C_{bridge} bond (1.385(2) Å) is significantly shorter than the N–C_{Ar} bonds (1.440(2), 1.441(2) Å); the bridging arylene group exhibits a slightly quinoidal pattern of bond lengths with a difference of *ca.* 0.033(3) Å between the bonds that are formally double and single in the zwitterionic structure shown in Fig. 4b (differences of *ca.* 0.1 Å are found in fully quinoidal structures[49]); the vinylene portion of the bridge shows a bond-length alternation (BLA) between formally double and single bonds of *ca.* 0.079(6) Å, a little lower than the >0.1 Å found for –CH=CH– groups (including those linking aryl and thienyl groups) in the absence of significant zwitterionic contributions;[50–52] and the formally double (1.384(2) Å, 1.414(2) Å) and single (1.386 Å) C–C bonds in the thiophene ring are very similar in length, in contrast to the strongly alternating pattern found in the absence of strong donor and acceptor substitution.[50–52] The patterns of bond lengths in **1** are similar to those seen in the structure of other related donor–acceptor chromophores with strong π-acceptors, such as **IV** (Fig. 4c).[53,54]

The relative contributions of neutral and zwitterionic resonance structures, which can be described in terms of the BLA between formally single and double bonds in polyenic parts of molecules, determine the magnitudes of the linear and nonlinear polarisabilities:[22,23,55–57] the linear polarisability, α, is maximised at zero BLA; β exhibits positive and negative peaks at BLA of *ca.* 0.05 and −0.05 Å, respectively,[58] and is zero at BLA = 0; and γ exhibits positive peaks at ±0.06–0.085 Å,[59] a negative peak at 0, and vanishes at ±0.04 Å.[22] The structural data, together with NMR data indicating a fairly large ^1H–^1H coupling constant for the vinylene protons (see experimental section), suggests that the neutral resonance structure is most important for **1**, but with sufficient zwitterionic contributions to give a BLA close to that corresponding to one of the positive maxima in γ, and somewhat higher (more neutral-dominated) than that at which the positive maximum in β is expected.

The packing in the structure of **1** is fairly complex; however, like the structures of many other strongly dipolar chromophores, the crystal can be viewed as being built of π-stacked dimers in which the principal axes of the molecules are antiparallel to one another. In the case of **1**, both pairs of molecules related to one another by inversion and pairs related by rotation can be identified. The molecules in the non-centrosymmetric pair generated by rotation are closest to one another and are characterised by π-stacking (interplanar distance of *ca.* 3.3 Å) between the tricyanovinylthiophene group and the phenylenevinylene moiety of the neighbouring chromophore (and *vice versa*). In addition to π-stacking intermolecular interactions, several intra- and interdimer C≡N···H–C contacts of *ca.* 2.7 Å are found in the structure; these types of interactions are also present in the structures of **IV**[53] and of many other cyano compounds.[60–64] The structure also exhibits an interdimer π interaction between carbon atoms on neighbouring aryl groups, and an interdimer distance of 2.9 Å between an alkyl H atom and one of the carbon atoms (C18) of the bridging arylene group.

Linear spectroscopy

Linear absorption spectra for **1** in selected solvents are shown in Fig. 5. The absorption maxima show only a weak dependence on the solvent polarity, although the bandshape is rather different in the low polarity solvent cyclohexane, in which it appears to

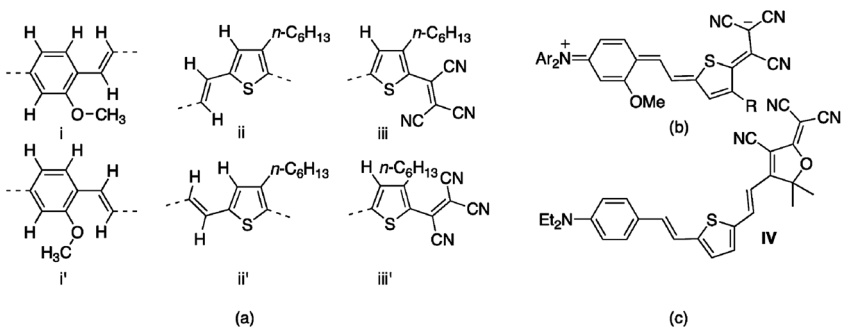

Fig. 4 (a) Possible conformations for different parts of chromophore **1**; (b) zwitterionic resonance structure for chromophore **1**; and (c) a crystallographically characterised chromophore, **IV**, related to **1**.

display poorly resolved vibronic structure, from that seen in more polar solvents, where a structureless approximately Gaussian profile is found. Typically strong positive solvatochromism is observed for simple donor–acceptor polyenes in which the ground-state structure is dominated by the neutral resonance structure; the less pronounced solvatochromism of **1** is perhaps attributable to the competing solvation of the dipole associated with the main donor–acceptor axis and that of local dipoles associated with the polar substituents, and, to some extent, to the effects of the bulky alkyl substituents. The spectrum of **1** in dichloromethane (not shown, $\lambda_{max} = 690$ nm) is very similar to that for its close analogue **I** in the same solvent ($\lambda_{max} = 696$ nm).[9]

The solution UV-vis spectra of **1** are similar to those of thin films of **1** and **1**-containing polymer composites (see ref. 24 for the spectrum of a 20 wt% blend of **1** in polystyrene). As we have previously noted,[24] the linear spectra show some desirable characteristics for applications involving frequency tripling at 1.5 μm: the intense low-energy absorption is anticipated to lead to a strong dispersion enhancement of $\chi^{(3)}(-3\omega;\omega,\omega,\omega)$ at this wavelength, while the low-energy band lies sufficiently high in energy to avoid impairing linear transparency at the fundamental wavelength; furthermore, the transparency at the third harmonic is also reasonably good, with a minimum in the absorption spectrum approximately corresponding to this wavelength.

Table 2 compares the absorption maxima, peak absorptivities, and transition dipole moments, μ_{ge}, for the low-energy absorptions of **1–3** in THF. The bathochromic shifts seen for **2** can be attributed to the longer total conjugation length associated with its acceptor group, and to the inductive effect of the SO_2 group increasing the acceptor strength.[65] The small additional bathochromic shift found for **3** is consistent with previously reported data recorded in dichloromethane,[20] and presumably reflects the outcome of a competition between the effects of a longer conjugation path in **2** and better donor–acceptor coupling through the polyene bridge of **3** than through the thiophene-containing bridge of **2**. The values of μ_{ge} for **2** and **3** are larger than that of **1**, consistent with the known effects on μ_{ge} of increasing the conjugation length.[66] The increased acceptor strength is also likely to play a role by reducing the BLA; μ_{ge} is predicted to increase as the BLA is decreased to zero and then to decrease again.[67,68] The similar values of μ_{ge} for **2** and **3** presumably result from cancellation of the opposing effects of conjugation length and BLA.[69]

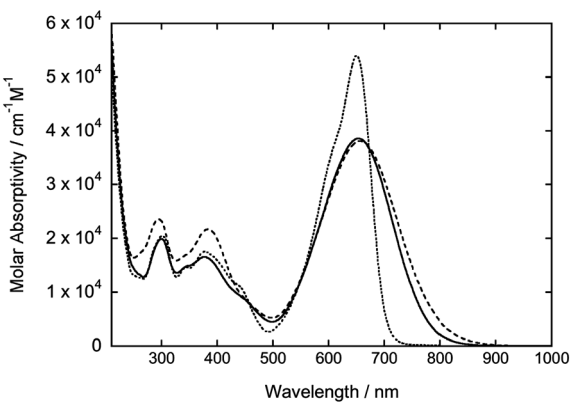

Fig. 5 Solution UV-vis spectra of **1** in cyclohexane (dotted line), THF (solid line), and acetonitrile (dashed line).

Table 2 One- and two-photon[a] absorption peak transition energies, transition dipole moments, and peak non-degenerate two-photon cross-sections[a] for **1–3** in THF

Compound	E_{1PA}/eV	ε_{max}/ 10^3 M^{-1} cm^{-1}	μ_{ge}[b]/D	E_{2PA}[c]/eV	δ_{max}/GM
1	1.90	38.6	9.4	1.82	290
2	1.75	48.9	11.1	1.78	240
3	1.67	60.0	11.9	1.82	290

[a] Measured by the WLC pump–probe method using a pump wavelength of 1800 nm. 1 GM = 1×10^{-50} cm^4 s photon^{-1}. Errors associated with experimentally-determined δ values are ±15%. [b] Estimated by integration of the low-energy absorption band according to $\mu_{ge} = 0.09584 \times [\int(\varepsilon/\nu)d\nu]^{0.5}$ where ε and ν are in M^{-1} cm^{-1} and cm^{-1}, respectively. [c] Note that the transition energy is equal to the sum of the energies of the two absorbed photons.

Nonlinear spectroscopy

Non-degenerate 2PA spectra (Fig. 6) were acquired for **1** in THF solution and in a film of **1** using the white-light continuum (WLC) pump–probe method.[70] The solution 2PA maximum and peak cross-section, δ_{max}, for **1** are compared with those obtained for **2** and **3** using the same method in Table 2 (the 2PA spectra are shown in the ESI). Degenerate 2PA cross-sections, δ, for **1** were also acquired at selected wavelengths using the open-aperture Z-scan technique.[71,72] Values of cross-sections from both techniques for samples of **1** in various media are shown in Table 3; in general these values obtained from different techniques and for different samples are in good agreement with one another. Such good agreement is not necessarily an obvious

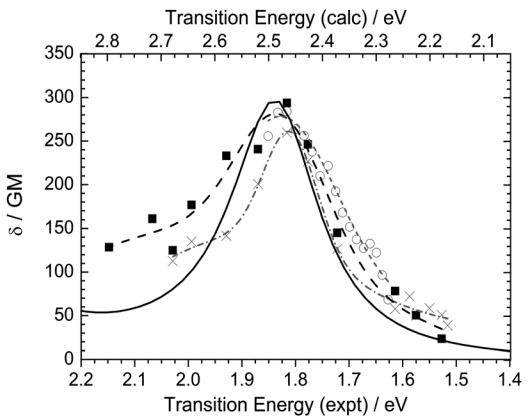

Fig. 6 Non-degenerate 2PA spectra acquired using the WLC pump–probe method in THF solution with a pump wavelength of 1800 nm (solid squares, long dashes) or 1550 nm (open circles, short dashes) or on a film (20 wt% in polycarbonate) using a pump wavelength of 1800 nm (crosses, dash-dotted) compared to the spectrum simulated from quantum-chemical calculations (solid line, note the offsets between *x*-axes for experimental and theoretical data). Lines used for experimental data are meant as guides for the eye. 1 GM = 1×10^{-50} cm^4 s photon^{-1}. Errors associated with experimentally-determined δ values are ±15%.

Table 3 Non-degenerate (using a 1800 nm pump) and degenerate two-photon cross-sections at a transition energy of 1.91 eV (equivalent to a degenerate photon wavelength of 1300 nm) for solution and films of **1** acquired using the WLC pump–probe and open-aperture Z-scan method, respectively

Sample	Method	δ/GM
THF solution	WLC, 1800 nm pump	240
THF solution	Z-scan	210
20 wt% in PC[a]	WLC, 1800 nm pump	160
20 wt% in PC[a]	Z-scan	210
1 wt% in PS[b]	Z-scan	240
free-standing film, 20 wt% in PC[a]	Z-scan	200
free-standing film, 20 wt% in PS[b]	Z-scan	320

[a] PC = polycarbonate. [b] PS = polystyrene. 1 GM = 1×10^{-50} cm^4 s photon^{-1}. Errors associated with experimentally-determined δ values are ±15%.

outcome and requires further explanation. The use of non-degenerate excitation is known to give rise to enhancement of the resulting 2PA cross-sections, δ_{ND}, over those acquired *via* degenerate excitation.[73] Such intermediate-state resonance enhancement might lead one to expect disparate WLC pump–probe and Z-scan results. For the case of unsymmetrical donor–acceptor chromophores, 2PA into the first excited state (which is also one-photon allowed) is often well-described by a two-state term (see below). In that case, the magnitude of this enhancement can be estimated (see eqn (3) in ref. 73) from the ratio between the degenerate photon energy, $\hbar\omega_D$, to that of the lower energy photon in the non-degenerate case, $\hbar\omega_{ND}$, *i.e.*,

$$\delta_{ND}/\delta_{ND} = \hbar\omega_D/\hbar\omega_{ND} \quad (1)$$

From Fig. 6, these values can be extracted for measurements of **1** in solutions of THF: $\hbar\omega_D = 0.91$ eV, $\hbar\omega_{ND(1500)} = 0.80$ eV, and $\hbar\omega_{ND(1800)} = 0.69$ eV; consequently, at most an enhancement of only *ca.* 30% should be expected; this is fully consistent with the similarities observed between the non-degenerate spectra in Fig. 6 and the values of δ in Table 3 from the two characterisation techniques. With regard to the characterisation of **1** in different media, the most significant difference between the various samples is the chromophore concentration, which varies from *ca.* 0.7 wt% in solution to 20 wt% in guest-host films. At such concentrations, aggregate-induced modifications to the linear and nonlinear optical properties might be expected. However, as discussed above, linear absorption spectra of **1** in dilute solutions (*ca.* 0.001 wt%) are quite similar to those of guest-host films (20 wt%) and neat thin films (100 wt%, see ref. 24); this suggests that aggregation effects on the 2PA properties of **1** should be similarly negligible, consistent with the results shown in Fig. 6 and Table 3.

It is often helpful to examine 2PA cross-sections in terms of essential-state models similar to those used to estimate hyperpolarisabilities. As noted above, for dipolar donor–acceptor chromophores in which the one-photon spectrum is dominated by a single transition, 2PA excitation from the ground state, g, into that excited state, e, is often well-described using the two-state expression:

$$\delta_{max} \propto \mu_{ge}^2 \Delta\mu_{ge}^2/\Gamma \quad (2)$$

where μ_{ge} is the transition dipole moment, $\Delta\mu_{ge}$ is the change in state dipole moment associated with the transition, and Γ is a damping factor associated with the transition linewidth. As noted above, crystallographic and NMR data indicate a fairly large positive BLA for **1**, suggesting significant $\Delta\mu_{ge}$ (the evolution of $\Delta\mu_{ge}$ with BLA is shown in ref. 68), which, in combination with the moderately large value of μ_{ge}, is anticipated to give rise to a significant two-photon cross-section for this state.

Quantum-chemical calculations of the linear and nonlinear absorption properties of **1** (disregarding effects due to the surrounding medium, see experimental section) are in excellent agreement with conclusions from experiment once allowance is made by the tendency of the method to overestimate transition energies; calculated values of $E_{ge} = 2.48$ eV and $\mu_{ge} = 10.9$ D can be compared with the experimental values in Table 2, while the calculated value of $\Delta\mu_{ge} = 12.1$ D is consistent with the expectations discussed in the previous paragraph. Fig. 6 superimposes experimental and calculated 2PA data, plotted with a damping of 0.1 eV, chosen to give a similar absorption linewidth to the experimental data, with the *x*-axes offset according to the discrepancy between the experimental and calculated 1PA transition energies.

Consistent with the similar linear absorption maxima for **1–3**, all three compounds exhibit similar 2PA maxima and peak cross-sections. The effects of a larger value of μ_{ge} in **2** than in **1** are presumably more than cancelled out by a smaller value of $\Delta\mu_{ge}$ associated with the stronger donor–acceptor coupling (reduced BLA). The shorter conjugation length and reduced BLA in **3** relative to **2** (see above) are expected to give an even smaller $\Delta\mu_{ge}$. However, despite this and the similarity of μ_{ge} to that of **2**, δ_{max} for **3** is somewhat larger than for **2**; this is likely to be due to a narrower absorption bandwidth (equivalent to a reduced Γ) in the 2PA spectrum of **3**, consistent with what is also seen in the 1PA spectra (see ESI).

The peak values of δ for **1–3** are somewhat higher than previously reported for a range of stilbenes and azobenzenes with amino donors and cyano or nitro acceptors,[74] *i.e.*, chromophores with similar conjugation lengths to **1**, but with electronic structures more dominated by the neutral resonance structure. In that study, the highest peak cross-section, *ca.* 200 GM (1 GM = 1×10^{-50} cm^4 s photon^{-1}), was reported for *E*-4-(dimethylamino)-4′-nitrostilbene.[74] The 2PA maximum for **1** is observed at a considerably longer photon wavelength (*ca.* 1370 nm[75] *vs. ca.* 900 nm for *E*-4-(dimethylamino)-4′-nitrostilbene) as anticipated from its low-energy 1PA maximum and consistent with the stronger acceptor, the replacement of a phenylene with a less aromatic thienylene, and the slightly longer conjugation length. In this context it should, however, be pointed out that other dipolar chromophores with longer conjugation paths between donor and acceptor have been found to exhibit considerably higher cross-sections (which are also higher when expressed on a per π-electron basis) into the low-energy 1PA state.[76,77]

We have also measured values of Re[$\gamma(-\omega;\omega,-\omega,\omega)$] – the molecular quantity relevant for AOS applications that take advantage of the intensity-dependent refractive indices of $\chi^{(3)}$ materials – for films containing **1** (Fig. 7a) using the closed-aperture Z-scan technique.[71,72,78] Some of the experimental values

of Re[$\gamma(-\omega;\omega,-\omega,\omega)$] (*e.g.* a value of 9.0×10^{-33} esu for the polycarbonate film at a photon wavelength 1500 nm) are fairly large compared to other compounds with sizable nonlinearities in this spectral range.[1,3,5,79] However, for use in AOS applications, linear and nonlinear transparency is required at the relevant wavelengths. While films of **1** show excellent *linear* transparency in the telecommunications region, the 2PA resonance that leads to the enhanced values of Re[$\gamma(-\omega;\omega,-\omega,\omega)$] in this range (*vide infra*) is also responsible for significant nonlinear optical losses. This gives rise to poor two-photon figures-of-merit[5] Re[$\gamma(-\omega;\omega,-\omega,\omega)$]/Im[$\gamma(-\omega;\omega,-\omega,\omega)$], the highest value being 3.7 for the polycarbonate film at 1500 nm.

Fig. 7a also plots the dispersion of Re[$\gamma(-\omega;\omega,-\omega,\omega)$] obtained from quantum-chemical calculations (using the same damping energy used for the theoretical 2PA spectrum in Fig. 6 and again with offset *x*-axes to allow for the theoretical overestimation of transition energies); this clearly shows that the experimental values are affected by substantial 2PA resonant enhancement. At longer wavelengths, Re[$\gamma(-\omega;\omega,-\omega,\omega)$] falls away to give much smaller values than those found in the telecommunications range (with the zero-frequency limit being calculated to be 175×10^{-36} esu). The overall form of the dispersion is broadly consistent with the wavelength dependence of the experimental data, reproducing the change in sign for Re[$\gamma(-\omega;\omega,-\omega,\omega)$] observed within the experimental photon energy range 0.85–0.90 eV; however, the peak values suggested by theory (using $\Gamma = 0.1$ eV) are considerably smaller than those obtained by experiment.[80]

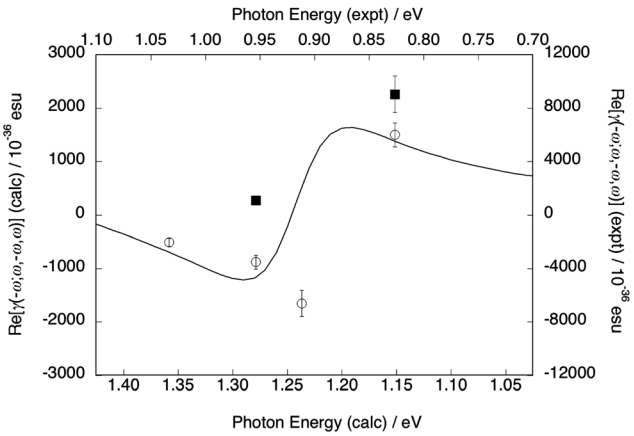

(a)

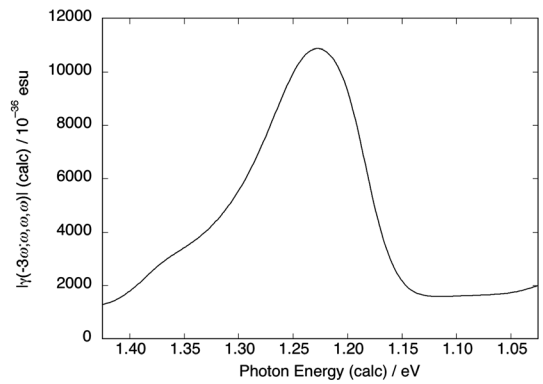

(b)

Fig. 7 Third-order polarisability for **1**: (a) theoretical dispersion of Re[$\gamma(-\omega;\omega,-\omega,\omega)$] (solid line) compared to experimental Z-scan measurements of Re[$\gamma(-\omega;\omega,-\omega,\omega)$] obtained for freestanding films containing 20 wt% of **1** in polycarbonate (filled squares) or polystyrene (open circles); (b) theoretical dispersion of the absolute magnitude of $\gamma(-3\omega;\omega,\omega,\omega)$. Note the different scales for experimental and theoretical data in (a). Note that the photon energy ranges plotted correspond to the transition energy ranges shown in Fig. 6 for the case of degenerate 2PA. 1 esu = cm^5 statVolt^{-2}. Errors associated with experimentally-determined γ values are ±15%. The calculated dispersions are shown for a more extensive wavelength range in the ESI.

Fig. 7b shows the theoretical dispersion of the absolute magnitude of $\gamma(-3\omega;\omega,\omega,\omega)$ – the molecular quantity responsible for THG – calculated with the same damping used for the theoretical data shown in Fig. 6 and 7a. The peak of the response is calculated for a photon energy of 1.23 eV, which is entirely consistent with 2PA resonant enhancement expected at this energy (see Fig. 6 and 7a). When this curve is corrected for the theoretical overestimation of transition energies, a peak in the experimental $\gamma(-3\omega;\omega,\omega,\omega)$ value corresponding to an experimental photon energy of 0.90 eV (wavelength of 1380 nm) is expected, close to the measured 2PA absorption maximum. This differs from an experimental spectrum of THG power for a **1** (20 wt%) / polystyrene film shown in ref. 26, in which the maximum is at *ca.* 1550 nm (0.80 eV) and the value at 1380 nm is much lower; however, the experimental spectrum may suffer from complications arising from 2PA of the fundamental and 1PA of the third harmonic at higher photon energies thereby bathochromically shifting the expected peak of the THG efficiency curve.[81]

Summary

We have described the synthesis of a chromophore that has been found to exhibit utility in THG-based applications. The X-ray crystal structure shows bond length patterns consistent with the observed third-order nonlinearities and indicates that weak intermolecular hydrogen bonding plays an important role in determining the structure. Z-scan data indicate that this compound, along with closely related dipolar compounds with similar absorption maxima, exhibits moderate near-infrared two-photon absorption. The real part of the third-order polarisability approaches 10^{-32} esu at *ca.* 1500 nm due to the two-photon resonance.

Experimental

General

THF and Et_2O for use in water-sensitive reactions were distilled from sodium benzophenone ketyl prior to use. DSC and TGA were acquired using a TA Instruments DSC Q200 and a NETZSCH STA 449C, respectively. Cyclic voltammetry was carried out under nitrogen on dry deoxygenated dichloromethane solutions *ca.* 5×10^{-4} M in analyte and 0.1 M in tetra-*n*-butylammonium hexafluorophosphate using a BAS Potentiostat, a glassy carbon working electrode, a platinum auxiliary electrode, and, as a pseudo-reference electrode, a silver wire anodised in 1 M aqueous potassium chloride. Ferrocene or decamethylferrocene ($E_{1/2}^{+/0} = -0.55$ V *vs.* $FeCp_2^{+/0}$) were used

as an internal reference. UV-vis spectra were recorded using a Varian Cary 5E spectrometer and 1 cm cuvettes.

4-(Bis(4-*n*-butylphenyl)amino)-2-methoxybenzaldehyde (5)

An oven-dried three-necked round-bottomed flask equipped with magnetic stirbar, thermometer, bubbler and nitrogen inlet was charged with compound **4**[9] (8.41 g, 21.7 mmol). Anhydrous DMF (1.5 eq, 32.55 mmol, 2.38 g) was added under the atmosphere of nitrogen followed by addition of $POCl_3$ (3.99 g, 26.0 mmol, 1.2 eq). The reaction mixture turned red-brown and the internal temperature increased up to 85 °C due to the exothermicity of the reaction. The mixture was then heated with stirring for 3 h (90–92 °C oil bath temperature) and then allowed to cool to room temperature and treated with aqueous NaOH solution (4.0 g in 100 mL of water). The resulting dark gum was stirred with Et_2O (30 mL) and transferred to a separatory funnel; additional Et_2O (50 mL) was added and the organic phase was separated. The aqueous phase was extracted with additional Et_2O (3 × 40 mL). The combined organic phases were washed with brine, dried over $MgSO_4$, and filtered; the solvent was then removed using rotary evaporation. The crude product was purified by column chromatography (500 mL of silica gel, hexanes:EtOAc = 10 : 1 as eluant) to give a bright yellow thick oil (7.04 g, 78%). ^{1}H NMR (400 MHz, $CDCl_3$): δ 10.19 (s, 1H), 7.62 (d, J = 8.7 Hz, 1H), 7.14 (d, J = 8.5 Hz, 4H), 7.09 (d, J = 8.5 Hz, 4H), 6.46 (dd, J = 8.7 Hz, 2.0 Hz, 1H), 6.37 (d, J = 2.0 Hz, 1H), 3.67 (s, 3H), 2.60 (t, J = 7.8 Hz, 2H), 1.61 (m, 4H), 1.37 (m, 4H), 0.94 (t, J = 7.3 Hz, 6H). ^{13}C{^{1}H} NMR (100 MHz, $CDCl_3$): δ 187.58 (CHO quaternary), 163.19 (quaternary), 155.26 (quaternary), 143.60 (quaternary), 140.10 (quaternary), 129.85 (CH), 129.54 (CH), 126.48 (CH), 117.72 (quaternary), 111.35 (CH), 100.74 (CH), 55.35 (MeO CH_3), 35.12 (CH_2), 33.47 (CH_2), 22.37 (CH_2), 13.89 (CH_3) (assignment made using a DEPT 135 experiment). HRMS (EI) calcd for $C_{28}H_{33}NO_2$: 415.2511; found: 415.2505. Anal. Calc. for $C_{28}H_{33}NO_2$: C, 80.93; H, 8.00. Found: C, 81.07; H, 8.15.

2-(Trimethylsilyl)-3-bromothiophene (8)

LDA (87.5 mL of a 1.8 M solution in THF / *n*-heptane, 158 mmol) was added over 30 min to a solution of 3-bromothiophene (24.46 g, 150 mmol) in anhydrous THF (100 mL) cooled in an acetone / dry ice bath (internal temperature −63 to −55 °C). A thick suspension formed after stirring for 5 min. The reaction mixture was stirred for 1.5 h and Me_3SiCl (17.11 g, 1.05 eq) was added slowly. The mixture was allowed to warm up to room temperature and water (50 mL) was added. The organic phase was separated, and the aqueous phase was extracted with hexanes (3 × 10 mL). The combined organic extracts (greenish-yellow) were dried over $MgSO_4$. The drying agent was filtered off and the solvents were removed by rotary evaporation. The crude product was isolated as dark yellow-orange oil; vacuum distillation (b.p. 56 °C, <2 mmHg) gave the product as a colorless oil (29.0 g, 82%). The ^{1}H NMR spectrum was consistent with literature data for **8** prepared using an alternative method starting from 2,3-dibromothiophene.[82]

2-(Trimethylsilyl)-3-*n*-hexylthiophene (9)

n-Hexylmagnesium bromide (60 mL of a commercial 2.0 M solution in diethyl ether, 1.2 eq, 0.12 mol) was added over 3 h period to a mixture of **8** (0.10 mol, 23.52 g), catalyst $NiCl_2$(dppp) (1.08 g, 2 mmol, 2 mol%), and anhydrous THF (100 mL). During the addition of the Grignard reagent the catalyst dissolved, the flask became warm to the touch, and precipitate formed. The orange-brown reaction mixture was stirred for 1 h, quenched by the addition of aqueous NH_4Cl (a few mL), and then treated with water (50 mL); the organic phase was separated and passed through a pad of silica gel (*ca.* 5 cm thick), eluting with hexanes (300 mL). The resulting solution was dried over $MgSO_4$, the drying agent was removed by filtration, the solvent was removed under reduced pressure, and the resulting yellow-orange oil subjected to fractional vacuum distillation (b.p. 93–95 °C, <2.0 mmHg) to give the product as a colorless oil (19.50 g, 81%). ^{1}H NMR (400 MHz, $CDCl_3$): δ 7.45 (d, J = 4.6 Hz, 1H), 7.1 (d, J = 4.7 Hz, 1H), 2.7 (poorly resolved t, 2H), 1.59 (m, 2H), 1.40–1.30 (m, 6H), 0.90 (t, J = 6.5 Hz, 3H), 0.35 (s, 9H); ^{13}C{^{1}H} NMR (100 MHz, $CDCl_3$): δ 150.35, 132.34, 130.18, 129.22, 31.69, 31.64, 31.12, 29.30, 22.50, 13.96, 0.23. The ^{1}H NMR data are in agreement with the spectrum shown in the literature.[83]

4-*n*-Hexyl-5-trimethylsilanyl-thiophene-2-carbaldehyde (10)

A solution of **9** (16.83 g, 70 mmol) in anhydrous THF (140 mL) was cooled in acetone / dry ice bath under an atmosphere of nitrogen and *n*-butyllithium (28 mL of a 2.5 M solution in hexanes, 0.070 mol) was added dropwise over 15 min (–70 to −63 °C internal temperature, exothermic reaction was observed). The mixture was stirred for 30 min and anhydrous DMF (9.15 g, 105 mmol, 1.5 eq) was added dropwise (–70 to −60 °C internal temperature, exothermic reaction). The cooling bath was removed and the very light yellow clear reaction mixture was allowed to warm up to room temperature. The reaction mixture was treated with NH_4Cl solution (10 g in 25 mL of water) and the organic solvents were removed by rotary evaporation. The residue was treated with hexanes (30 mL), the organic phase was removed and the aqueous phase was extracted with hexanes (3 × 10 mL). The combined organic extracts (yellow) were dried over $MgSO_4$ and filtered; the solvent was then removed by rotary evaporation and the resulting material was subjected to Kugelrohr distillation (150–160 °C, <2 mmHg) to give the product as a yellowish oil (13.93 g, 74%). Analytically pure compound was obtained as yellowish oil after purification by column chromatography (silica gel, hexanes/EtOAc (10 : 1) as eluant). ^{1}H NMR (400 MHz, $CDCl_3$): δ 9.85 (s, 1H), 7.64 (s, 1H), 2.65 (t, J = 7.9 Hz, 2H), 1.60 (m, 2H), 1.40–1.25 (m, 6H), 0.87 (t, J = 6.8 Hz, 3H), 0.35 (s, 9H). ^{13}C{^{1}H} NMR (100 MHz, $CDCl_3$): δ 182.41, 151.18, 146.58, 145.99, 138.04, 31.63, 31.46, 31.07, 29.21, 22.53, 14.00, −0.11. HRMS (EI) calcd for $C_{14}H_{24}OSSi$: 268.1317; found: 268.1259. Anal. Calc. for $C_{14}H_{24}OSSi$: C, 62.63; H, 9.01. Found: C, 62.88; H, 8.99.

(4-*n*-Hexyl-5-trimethylsilanyl-thiophen-2-yl)-methanol (11)

The preparation of **11** was based on a published procedure for a similar substrate.[84] Compound **10** (9.40 g, 35 mmol) was dissolved in EtOH (130 mL) and $NaBH_4$ (2.66 g, 70.35 mmol, 2.01 eq) was added in portions at room temperature over a 20 min period. The mixture was stirred for 1 h, cooled in ice-water bath and acetone (10 mL) was added dropwise. The solvents were

removed by rotary evaporation, the residue was treated with brine (50 mL), hexanes (50 mL), and EtOAc (10 mL). The organic phase was separated and the aqueous phase was extracted with EtOAc (4 × 10 mL). The combined organic phases were dried over $MgSO_4$, the drying agent was filtered off, and the solvents were removed by rotary evaporation. The residual solvent was removed under vacuum, leaving the product as a yellowish oil (9.15 g, 97% yield). ^{1}H NMR (400 MHz, $CDCl_3$): δ 6.95 (s, 1H), 4.77 (s, 2H), 2.00–1.90 (broad s, 1H), 1.55 (m, 2H), 1.40–1.20 (m, 6H), 0.89 (t, $J = 6.9$ Hz, 3H), 0.35 (s, 9H). ^{13}C{^{1}H} NMR (100 MHz, $CDCl_3$): δ 150.52, 147.74, 133.12, 128.97, 59.96, 31.71 (two CH_2), 31.41, 29.38, 22.58, 14.05, 0.31. HRMS (EI) calcd for $C_{14}H_{26}OSSi$: 270.1474; found: 270.1400. Anal. Calc. for $C_{14}H_{26}OSSi$: C, 62.16; H, 9.69. Found: C, 62.35; H, 9.76.

(4-*n*-Hexylthiophen-2-yl)-methanol (12)

The preparation of **12** was based on a published procedure for a similar substrate.[85] Compound **11** (23 mmol, 6.22 g) was dissolved in anhydrous THF (10 ml) and a solution of ^{n}Bu$_4$NF (46 mL of a 1 M solution in THF, 46 mmol, 2 eq) was added. The mixture was stirred for 2 d (when starting material was no longer detectable using GCMS). The mixture was treated with aqueous NH_4Cl (6 g in 25 mL of water), the organic phase was separated, and the aqueous phase was extracted with EtOAc (3 × 10 mL). The combined organic phases were washed with brine, then dried over $MgSO_4$. After filtration, the solvents were removed by rotary evaporation and the resulting thick cloudy yellow oil was purified by column chromatography (150 mL of silica gel, eluting with hexanes / EtOAc (10 : 1 and then 5 : 1)) to give the product as a yellowish oil (3.5 g, 77% yield). The ^{1}H NMR spectrum was consistent with that previously reported.[9]

(4-*n*-Hexyl-thiophen-2-yl)-methyltriphenylphosphonium chloride (6)

The phosphonium salt **6** was prepared from **12** as previously described.[9,86]

E-2-Tricyanovinyl-3-*n*-hexyl-5-[4-{bis(4-*n*-butylphenyl)amino}-2-methoxystyryl]-thiophene (1)

A solution of sodium ethoxide was prepared by the addition of small pieces of Na (0.53 g, 23 mmol, 1.5 eq) to EtOH (25 mL) and was then added dropwise to a solution of phosphonium salt **6** (5.51 g, 11.5 mmol) and aldehyde **5** (4.78 g, 11.5 mmol) in EtOH (80 mL). The reaction mixture was heated to reflux for 1 h, after which TLC indicated no remaining aldehyde; the mixture was allowed to cool to room temperature, treated with water, and extracted with Et_2O. The combined organic extracts were dried over $MgSO_4$; the drying agent was filtered off and the solvent was removed by rotary evaporation. The residue was purified by column chromatography (silica gel, hexanes / EtOAc (20 : 1)), the solvents were removed by rotary evaporation; the resultant intermediate **7** – a thick yellow oil – was used immediately in the next step without further purification and characterisation. **7** was redissolved in anhydrous DMF (50 mL) and TCNE (2.95 g, 23 mmol, 2 eq, purified by sublimation prior to use) was added in one portion under nitrogen. The mixture was heated to 55 °C. After 6 h, TLC showed some remaining **7**; additional TCNE (0.75 g, *ca.* 0.5 eq) was added and the mixture stirred for an additional 15 h at 55 °C under nitrogen. A very dark reaction mixture was cooled to room temperature, treated with brine and Et_2O (100 mL); the organic phase was separated and the aqueous phase was extracted with Et_2O (8 × 20 mL). The combined organic phases were dried over $MgSO_4$ and filtered; the solvent was then removed by rotary evaporation. The crude material was dissolved in EtOAc and filtered through silica gel (120 g, eluting with hexanes/acetone (100 : 1)). The solvent was removed by rotary evaporation, the sticky dark-green residue was dissolved in EtOAc, treated with 25 g of silica gel, the solvent was removed by rotary evaporation and this silica gel was applied to the top of a silica gel column (1 L, eluted with hexanes/EtOAc(100 : 1, then 50 : 1 then 25 : 1)). The first fractions were pure and produced a brown powder with a metallic lustre after removal of solvent by rotary evaporation (2.94 g). Additional fractions (2.2 g) were contaminated with a small amount of more polar impurity and were purified further using an additional column (300 mL of silica gel, eluting with hexanes/EtOAc (neat hexanes, then 100 : 1, then 50 : 1, and finally 30 : 1)). The residue obtained after solvent removal by rotary evaporation was dissolved in warm hexanes (20–25 mL) and the dark green solution was cooled to give a black solid with golden lustre after vacuum filtration (2.06 g). Total yield: 5.0 g (64% yield for two steps). ^{1}H NMR (400 MHz, $CDCl_3$): δ 7.48 (d, $J = 16.0$ Hz, 1H), 7.30 (d, $J = 8.7$, 1H), 7.16–7.10 (m, 5H), 7.07 (d, $J = 8.4$ Hz, 4H), 6.99 (s, 1H), 6.51 (dd, $J = 8.6$ Hz, 2.11 Hz, 1H), 6.47 (d, $J = 2.1$ Hz, 1H), 3.70 (s, 3H), 3.03 (t, $J = 7.9$ Hz, 2H), 2.60 (t, $J = 7.8$ Hz, 4H), 1.70–1.62 (m, 2H), 1.61–1.52 (m, 4H), 1.50–1.30 (m, 10H), 0.94 (t, $J = 7.3$ Hz, 6H), 0.90 (t, $J = 7.0$ Hz, 3H); ^{13}C{^{1}H} NMR (100 MHz, $CDCl_3$): δ 159.29, 158.20, 156.86, 151.78, 143.85, 139.47, 133.45, 129.77, 129.39, 129.29, 128.85, 125.91, 125.55, 116.52, 116.41, 113.73, 113.57, 113.44, 112.85, 102.32, 79.42, 55.34, 35.09, 33.53, 31.46, 31.32, 30.83, 29.10, 22.49, 22.39, 14.00, 13.95. HRMS(EI): calcd for $C_{44}H_{48}N_4OS$ (M^+): 680.3549; found: 680.3552. Anal. Calc. for $C_{44}H_{48}N_4OS$: C, 77.61; H, 7.11; N, 8.23. Found: C, 77.47; H, 7.12, N, 8.23. UV-vis (CH_2Cl_2) λ_{max} (ε_{max}) 690 (45000) nm ($M^{-1}cm^{-1}$).

X-ray crystallography

An irregular fragment (0.27 × 0.25 × 0.20 mm) of **1** ($C_{44}H_{48}N_4OS$, $M_w = 680.92$ g mol^{-1}) was found to belong to the monoclinic space group $C2/c$ with $a = 10.9857$ Å, $b = 15.0354(8)$ Å, $c = 46.669(3)$ Å, $\beta = 90.149(2)°$, $V = 7708.4(9)$ Å^3, $Z = 8$, $\rho_c = 1.173$ g cm^{-3}, and $\mu = 0.122$ mm^{-1}. A total of 30633 reflections (6815 independent) were measured over the θ range 0.87 to 25.05° at 100(2) K using a Bruker SMART APEX II diffractometer and Mo(Kα) radiation ($\lambda = 0.71073$ Å) radiation. The structure was solved by direct methods using SHELXS-97 and refined by full-matrix least-squares procedures on F^2 against all reflections using SHELXL-97;[87] SADABS[88] was used to apply an absorption correction and all hydrogen atoms were placed geometrically. Refinement converged with $R_1 = 0.0426$ and w$R_2 = 0.1266$ ($I > 2\sigma(I)$) and $R_1 = 0.0587$ and w$R_2 = 0.1430$ (all data). CCDC reference number 851132. For crystallographic data in CIF format see ESI.

Polymer-induced heteronucleation

Polymer-induced heteronucleation[44,45] studies of **1** were carried out using the same polymer libraries as described in the supporting information of ref. 43. Solutions of **1** in acetone (3.5 mM) were allowed to evaporate in the presence of these polymer libraries. Due to the high fluorescence of the material, Raman spectroscopy (exciting at 785 nm) was not useful in screening the material and, therefore, only optical microscopy and powder X-ray diffraction (as described in ref. 43), were used. Optical microscopy revealed that most of the crystals grew as orange clumps with a few well-defined crystals that had blade-like morphology. Powder X-ray diffraction patterns of samples from each library were all consistent with the pattern simulated from the known crystal structure.

Nonlinear optical characterisation

Doped films of chromophore **1** in various host polymers sandwiched between glass substrates employed for nonlinear optical characterisation were prepared according to a previously reported method.[24] Typical film thicknesses were on the order of 100 μm; while sandwiched films were adequate for determination of δ, free-standing films (*i.e.* films removed from substrates) were employed for determination of Re[$\gamma(-\omega;\omega,-\omega,\omega)$] *via* closed-aperture Z-scans so as to remove the contributions from the substrates. A linear refractive index of 1.59 was assumed for these films, consistent with values determined for the near-IR spectral region.[24] Finally, the density of the composite films was approximated to be 1 g cm^{-3} for the purpose of determining chromophoric concentrations. Concentrations of solutions used for nonlinear optical characterisation measurements were *ca.* 9 mM.

The general descriptions for the WLC pump–probe method[70,73] and the femtosecond-pulsed Z-scan technique[71,72] have been given previously; however, specific approaches and experimental parameters used for the work discussed herein are detailed in ref. 5 and 89 (for WLC pump–probe), and in ref. 5 and 90 (for Z-scan). Additionally, conversion from the macroscopic nonlinear optical parameters extracted from Z-scan measurements and the microscopic parameters discussed herein are given in ref. 90.

Quantum-chemical calculations

The geometry of an isolated **1** molecule was optimised at the B3LYP/6-31G* level[91] of density functional theory (DFT)[92–94] using Gaussian 03.[95] To calculate the ground- and excited-state electronic structure of **1**, we used the semi-empirical Intermediate Neglect of Differential Overlap (INDO) Hamiltonian[96] (spectroscopic parameterisation along with Mataga-Nishimoto[97] electron repulsion as implemented in the ZINDO code[98]) and coupled it to a multi-reference determinant configuration-interaction (MRDCI) scheme.[99,100] Accounting for electron correlations at an appropriate level (typically not provided by linear-response DFT) is especially important for the description of the 2PA active states[100–103] and also when calculating second-order nonlinear coefficients. The active space included the 34 highest occupied and 34 lowest unoccupied orbitals for singly excited determinants and the 6 highest occupied orbitals and 6 lowest unoccupied π-orbitals (the LUMO through LUMO+4 and the LUMO+7) for double excitations. The reference determinants comprised the SCF determinant, the HOMO → LUMO, HOMO−1 → LUMO, and HOMO → LUMO+1 singly-excited determinants, as well as the (HOMO,HOMO)→(LUMO, LUMO) doubly excited determinant. All non-linear optical properties were calculated following the approach by Orr and Ward;[104] $\gamma(-\omega;\omega,-\omega,\omega)$ and $\gamma(3\omega;\omega,\omega,\omega)$ were computed by using the perturbative Sum-over-States (SOS) expression including the 500 lowest-lying singlet excited states. The influence of the solvent or, more generally, the dielectric surrounding the molecules was not accounted for in the calculations; it should be borne in mind, however, that when calculating excitation energies and (transition) dipole moments solvent effects are implicitly included to some extent *via* the parametrisation of the INDO Hamiltonian. Finally, we note that in earlier computational work we typically reported hyperpolarisabilities following the Taylor series convention. Here, to be consistent with the way the experimental data are reported, we applied a power-series expansion of the polarisation response as a function of the applied field; this results in third-order polarisabilities that are smaller by a factor of six than for the Taylor series expansion.

Acknowledgements

This material is based upon work supported in part by the National Science Foundation STC Program under Agreement Number DMR-0120967 and the Defense Advanced Research Projects Agency (DARPA) MORPH Program and Office of Naval Research (N00014-04-0095 and N00014-06-1-0897). We are grateful to William Porter III and Adam Matzger (University of Michigan) for performing the polymer-induced heteronucleation experiments. We also thank Myoungsik Cha, Canek Fuentes-Hernandez, and Bernard Kippelen for fabrication of the guest-host films used in the nonlinear optical characterisation measurements.

References

1 J. M. Hales and J. W. Perry, in "*Introduction to Organic Electronic and Optoelectronic Materials and Devices*", ed. S.-S. Sun and L. Dalton, CRC Press, Orlando, 2008.
2 S. Polyakov, F. Yoshino, M. Liu and G. I. Stegeman, *Phys. Rev. B: Condens. Matter Mater. Phys.*, 2004, **69**, 115421.
3 J. M. Hales, S. Zheng, S. Barlow, S. R. Marder and J. W. Perry, *J. Am. Chem. Soc.*, 2006, **128**, 11362.
4 C. Koos, P. Vorreau, T. Vallaitis, P. Dumon, W. Bogaerts, R. Baets, B. Esembeson, I. Biaggio, T. Michinobu, F. Diederich, W. Freude and J. Leuthold, *Nat. Photonics*, 2009, **3**, 216.
5 J. M. Hales, J. Matichak, S. Barlow, S. Ohira, K. Yesudas, J.-L. Brédas, J. W. Perry and S. R. Marder, *Science*, 2010, **327**, 1485.
6 M. Samoc, A. Samoc and B. Luther-Davies, *Opt. Express*, 2003, **11**, 1787.
7 S.-H. Chi, J. M. Hales, C. Fuentes-Hernandez, S.-Y. Tseng, J.-Y. Cho, S. A. Odom, Q. Zhang, S. Barlow, R. R. Schrock, S. R. Marder, B. Kippelen and J. W. Perry, *Adv. Mater.*, 2008, **20**, 3199.
8 C. Fuentes-Hernandez, G. Ramos-Ortiz, S.-Y. Tseng, M. P. Gaja and B. Kippelen, *J. Mater. Chem.*, 2009, **19**, 7394.
9 S. Thayumanavan, J. Mendez and S. R. Marder, *J. Org. Chem.*, 1999, **64**, 4289.
10 S. R. Marder, B. Kippelen, A. K.-Y. Jen and N. Peyghambarian, *Nature*, 1997, **388**, 845.
11 L. R. Dalton, *J. Phys.: Condens. Matter*, 2003, **15**, R897.

12 C.-C. Chang, C.-P. Chen, C.-C. Chou, W.-J. Kuo and R.-J. Jeng, *J. Macromol. Sci., Polym. Rev.*, 2005, **45**, 125.
13 C. R. Moylan, R. J. Twieg, V. Y. Lee, S. A. Swanson, K. M. Betterton and R. D. Miller, *J. Am. Chem. Soc.*, 1993, **115**, 12599.
14 P. V. Bedworth, Y. M. Cai, A. Jen and S. R. Marder, *J. Org. Chem.*, 1996, **61**, 2242.
15 S. Ermer, S. M. Lovejoy, D. S. Leung, H. Warren, C. R. Moylan and R. J. Twieg, *Chem. Mater.*, 1997, **9**, 1437.
16 J. O. Morley, *J. Chem. Soc., Faraday Trans.*, 1991, **87**, 3009.
17 K. J. Drost, A. K.-Y. Jen and V. P. Rao, *Chemtech.*, 1995, **25**, 16.
18 I. D. L. Albert, T. J. Marks and M. A. Ratner, *J. Am. Chem. Soc.*, 1997, **119**, 6575.
19 E. M. Breitung, C.-F. Shu and R. J. McMahon, *J. Am. Chem. Soc.*, 2000, **122**, 1154.
20 Z.-Y. Hu, A. Fort, M. Barzoukas, A. K.-Y. Jen, S. Barlow and S. R. Marder, *J. Phys. Chem. B*, 2004, **108**, 8626.
21 G. Bourhill, B. G. Tiemann, J. W. Perry and S. R. Marder, *Nonlinear Optics*, 1995, **10**, 49.
22 C. B. Gorman and S. R. Marder, *Chem. Mater.*, 1995, **7**, 215.
23 S. R. Marder, C. B. Gorman, F. Meyers, J. W. Perry, G. Bourhill, J.-L. Brédas and B. M. Pierce, *Science*, 1994, **265**, 632.
24 G. Ramos-Ortiz, M. Cha, S. Thayumanavan, J. C. Mendez, S. R. Marder and B. Kippelen, *Appl. Phys. Lett.*, 2004, **85**, 179.
25 G. Ramos-Ortiz, M. Cha, S. Thayumanavan, J. Mendez, S. R. Marder and B. Kippelen, *Appl. Phys. Lett.*, 2004, **85**, 3348.
26 G. Ramos-Ortiz, M. Cha, B. Kippelen, G. A. Walker, S. Barlow and S. R. Marder, *Opt. Lett.*, 2004, **29**, 2515.
27 G. Ramos-Ortiz, M. Cha, S. Barlow, G. Walker, S. R. Marder and B. Kippelen, *Proc. S.P.I.E., Int. Soc. Opt. Eng.*, 2004, **5622**, 439.
28 G. Ramos-Ortiz, M. Cha, B. Kippelen, G. A. Walker, S. Barlow and S. R. Marder, *Trends in Optics and Photonics*, 2004, **96/A**, CTuI3/1.
29 C. W. Spangler, *J. Mater. Chem.*, 1999, **9**, 2013.
30 P.-A. Bouit, G. Wetzel, G. Berginc, B. Loiseaux, L. Toupet, P. Feneyrou, Y. Bretonnière, K. Kamada, O. Maury and C. Andraud, *Chem. Mater.*, 2007, **19**, 5325.
31 S. Tay, J. Thomas, M. Eralp, G. Li, B. Kippelen, S. R. Marder, G. Meredith, A. Schülzgen and N. Peyghambarian, *Appl. Phys. Lett.*, 2004, **85**, 4561.
32 S. Tay, J. Thomas, M. Eralp, G. Li, R. A. Norwood, A. Schülzgen, M. Yamamoto, S. Barlow, G. A. Walker, S. R. Marder and N. Peyghambarian, *Appl. Phys. Lett.*, 2005, **87**, 171105.
33 M. Ahlheim, M. Barzoukas, P. V. Bedworth, M. Blanchard-Desce, A. Fort, Z.-Y. Hu, S. R. Marder, J. W. Perry, C. Runser, M. Staehelin and B. Zysset, *Science*, 1996, **271**, 335.
34 M. Blanchard-Desce, V. Alain, P. V. Bedworth, S. R. Marder, A. Fort, C. Runser, M. Barzoukas, S. Lebus and R. Wortmann, *Chem.–Eur. J.*, 1997, **3**, 1091.
35 A. K. Y. Jen, Y. Cai, P. V. Bedworth and S. R. Marder, *Adv. Mater.*, 1997, **9**, 132.
36 A. K.-Y. Jen, V. P. Rao, K. J. Drost, K. Y. Wong and M. P. Cava, *J. Chem. Soc., Chem. Commun.*, 1994, 2057.
37 J. Ohshita, K.-H. Lee, M. Hashimoto, Y. Kunugi, Y. Harima, K. Yamashita and A. Kunai, *Org. Lett.*, 2002, **4**, 1891.
38 B. K. Spraul, S. Suresh, T. Sassa, M. Ángeles Herranz, L. Echegoyen, T. Wada, D. Perahia and D. W. Smith, *Tetrahedron Lett.*, 2004, **45**, 3253.
39 A decomposition temperature of 315 °C has been estimated for **II** using DSC (reference 35); however, we have previously noted that TGA tends to give lower, more conservative, estimates of decomposition temperature than DSC (ref. 41).
40 A. I. de Lucas, N. Martín, P. de Miguel, C. Seoane, A. Albert and F. H. Cano, *J. Mater. Chem.*, 1995, **5**, 1141.
41 K. Staub, G. A. Levina, S. Barlow, T. C. Kowalczyk, H. S. Lackritz, M. Barzoukas, A. Fort and S. R. Marder, *J. Mater. Chem.*, 2003, **13**, 825.
42 Specifically, a compound with the same donor as **1**, but in which the thiophene portion of the bridge is omitted, the alkene and part of the acceptor is incorporated in a ring, and where the acceptor is slightly weaker (dicyanovinyl in place of tricyanovinyl), is oxidised at $E_{1/2}$ = +0.46 V *vs.* ferrocenium/ferrocene in CH_2Cl_2. The increased potential *vs.* **1** presumably indicates stronger donor–acceptor coupling (decreased BLA); evidently the effects of a shorter conjugated bridge, omitting the aromatic thienylene group, outweighs the effect of a weaker acceptor. Other optical and electrochemical data in ref. 41 confirm that the 4-[bis(4-*n*-butylphenyl)amino]-2-methoxyphenyl group is a significantly stronger π-donor than 4-[bis(4-*n*-butylphenyl)amino]phenyl.
43 T. L. Kinnibrugh, S. Salman, Y. A. Getmanenko, V. Coropceanu, W. W. Porter, T. V. Timofeeva, A. J. Matzger, J.-L. Brédas, S. R. Marder and S. Barlow, *Organometallics*, 2009, **28**, 1350.
44 M. D. Lang, A. L. Grzesiak and A. J. Matzger, *J. Am. Chem. Soc.*, 2002, **124**, 14834.
45 C. P. Price, A. L. Grzesiak and A. J. Matzger, *J. Am. Chem. Soc.*, 2005, **127**, 5512.
46 X. Zhang, Z.-C. Li, K.-B. Li, F.-S. Du and F.-M. Li, *J. Am. Chem. Soc.*, 2004, **126**, 12200.
47 S. Barlow, C. Risko, V. Coropceanu, N. M. Tucker, S. C. Jones, Z. Levi, V. N. Khrustalev, M. Y. Antipin, T. L. Kinnibrugh, T. Timofeeva, S. R. Marder and J. L. Brédas, *Chem. Commun.*, 2005, 764.
48 S. C. Jones, V. Coropceanu, S. Barlow, T. Kinnibrugh, T. Timofeeva, J.-L. Brédas and S. R. Marder, *J. Am. Chem. Soc.*, 2004, **126**, 11782.
49 H. A. Staab, M. Jörns, C. Krieger and M. Rentzea, *Chem. Ber.*, 1985, **118**, 796.
50 D. Zobel, *Acta Crystallogr., Sect. B: Struct. Crystallogr. Cryst. Chem.*, 1976, **B32**, 2838.
51 D. Zobel and G. Ruban, *Acta Crystallogr., Sect. B: Struct. Crystallogr. Cryst. Chem.*, 1978, **B34**, 1652.
52 H. Irngartinger, J. Lichtenthaler and R. Herpich, *Struct. Chem.*, 1994, **5**, 283.
53 T. L. Kinnibrugh, T. V. Timofeeva, O. Clot, A. Akelaitis and L. R. Dalton, *Acta Crystallogr., Sect. E: Struct. Rep. Online*, 2006, **E62**, o4804.
54 For **IV** the N–C_{bridge} bond length is 1.371(3) Å, the phenylene ring shows a quinoidal bond length difference of 0.030(5) Å, the average BLA across the vinylene groups is 0.076(10) Å, and the C=C (1.382(3), 1.378(3) Å) and C–C (1.385(3) Å) bonds within the thienylene group are similar in length.
55 C. B. Gorman and S. R. Marder, *Proc. Natl. Acad. Sci. U. S. A.*, 1993, **90**, 11297.
56 S. R. Marder, J. W. Perry, G. Bourhill, C. B. Gorman, B. G. Tiemann and K. Mansour, *Science*, 1993, **261**, 186.
57 G. Bourhill, J.-L. Brédas, L.-T. Cheng, S. R. Marder, F. Meyers, J. W. Perry and B. G. Tiemann, *J. Am. Chem. Soc.*, 1994, **116**, 2619.
58 Here we define BLA as the difference between the average length of the polyene bonds that are formally single in the neutral resonance structure and the average length of those that are formally double, so that positive BLA corresponds to dominance by the neutral resonance structure and negative BLA to a predominantly zwitterionic structure. However, in some of the literature BLA is defined so that the opposite is true.
59 The precise positions of maxima depend on the chain length of the polyene system (ref. 22).
60 E. G. Popova, L. A. Chetkina and B. V. Kotov, *Zh. Strukt. Khim.*, 1976, **17**, 510.
61 T. V. Timofeeva, V. N. Nesterov, M. Y. Antipin, R. D. Clark, M. Sanghadasa, B. H. Cardelino, C. E. Moore and D. O. Frazier, *J. Mol. Struct.*, 2000, **519**, 225.
62 T. V. Timofeeva, G. H. Kuhn, V. V. Nesterov, V. N. Nesterov, D. O. Frazier, B. G. Penn and M. Y. Antipin, *Cryst. Growth Des.*, 2003, **3**, 383.
63 Y.-S. Yao, J. Xiao, X.-S. Wang, Z.-B. Deng and B.-W. Zhang, *Adv. Funct. Mater.*, 2006, **16**, 709.
64 Y.-P. Tian, L. Li, J.-Z. Zhang, J.-X. Yang, H.-p. Zhou, J.-y. Wu, P.-p. Sun, L.-m. Tao, Y.-h. Guo, C.-K. Wang, H. Xing, W.-h. Huang, X.-T. Tao and M.-H. Jiang, *J. Mater. Chem.*, 2007, **17**, 3646.
65 The different donor strengths may also play a role. However, the effects of exchanging 4-(dialkylamino)phenyl and 4-(diarylamino) phenyl vary considerably from system to system (compare data in ref. 21 and 41 for example), presumably because the energies of donor–acceptor charge-transfer transitions depend on *both* electron-transfer and π-donor characteristics of the donor groups, *i.e.*, the energy of donor-based orbitals and their ability to couple to the rest of the π-system; 4-(dialkylamino)phenyl is a stronger π-donor than 4-(diarylamino)phenyl, while the latter is the stronger electron-transfer donor, respectively (O. Kwon, S. Barlow, S. A. Odom, L. Beverina, N. J. Thompson, E. Zojer,

J.-L. Brédas and S. R. Marder, *J. Phys. Chem. A*, 2005, **109**, 9346).
66 In addition to the presence of an additional double bond in **2** between the donor and the dicyanovinylidene terminus of the acceptor influencing μ_{ge}, the fused benzene ring of this acceptor has previously been found to affect μ_{ge} much more significantly than λ_{max} (ref. 20) and so presumably helps contributes to the observed differences in μ_{ge} between **1** and **2/3**.
67 S. R. Marder, D. N. Beratan and L.-T. Cheng, *Science*, 1991, **252**, 103.
68 F. Meyers, S. R. Marder, B. M. Pierce and J.-L. Brédas, *J. Am. Chem. Soc.*, 1994, **116**, 10703.
69 Consistent with these arguments, the crystallographically determined BLA for the polyenic portion of **3** is *ca.* 0.04 Å (ref. 34), greatly reduced from that of **1**.
70 R. A. Negres, J. M. Hales, A. Kobyakov, D. J. Hagan and E. W. Van Stryland, *Opt. Lett.*, 2002, **27**, 270.
71 M. Sheik-bahae, A. A. Said and E. W. Van Stryland, *Opt. Lett.*, 1989, **14**, 955.
72 M. Sheik-bahae, A. A. Said, T.-H. Wei, D. J. Hagan and E. W. Van Stryland, *IEEE J. Quantum Electron.*, 1990, **26**, 760.
73 J. M. Hales, D. J. Hagan, E. W. V. Stryland, K. J. Schafer, A. R. Morales, K. D. Belfield, P. Pacher, O. Kwon, E. Zojer and J. L. Brédas, *J. Chem. Phys.*, 2004, **121**, 3152.
74 L. Antonov, K. Kamada, K. Ohta and F. S. Kamounah, *Phys. Chem. Chem. Phys.*, 2003, **5**, 1193.
75 It should be noted that larger cross-sections have been reported at telecommunications wavelengths for a variety of other chromophores including extended dipolar chromophores (ref. 77), extended squaraines (ref. 79), cyanines and merocyanines (P.-A. Bouit, G. Wetzel, G. Berginc, B. Loiseaux, L. Toupet, P. Feneyrou, Y. Bretonnière, K. Kamada, O. Maury and C. Andraud, *Chem. Mater.*, 2007, **19**, 5325), an extended bis (dithiolene) nickel complex (J.-Y. Cho, S. Barlow, S. R. Marder, J. Fu, L. A. Padilha, E. W. Van Stryland, D. J. Hagan and M. Bishop, *Opt. Lett.*, 2007, **32**, 671; J.-Y. Cho, J. Fu, L. A. Padilha, S. Barlow, E. W. Van Stryland, D. J. Hagan, M. Bishop and S. R. Marder, *Mol. Cryst. Liq. Cryst.*, 2008, **485**, 915) and several porphyrin-based materials (K. Kurotobi, K. S. Kim, S. B. Noh, D. Kim and A. Osuka, *Angew. Chem., Int. Ed.*, 2006, **45**, 3944; M. Drobizhev, Y. Stepanenko, A. Rebane, C. J. Wilson, T. E. O. Screen and H. L. Anderson, *J. Am. Chem. Soc.*, 2006, **128**, 12432).
76 K. D. Belfield, D. J. Hagan, E. W. Van Stryland, K. J. Schaefer and R. A. Negres, *Org. Lett.*, 1999, **1**, 1575.
77 L. Beverina, J. Fu, A. Leclercq, E. Zojer, P. Pacher, S. Barlow, E. W. V. Stryland, D. J. Hagan, J.-L. Brédas and S. R. Marder, *J. Am. Chem. Soc.*, 2005, **127**, 7282.
78 The definition of γ used here is that in which the dipole moment is expressed as a power series expansion in terms of the electric field: $\mu = \mu_0 + \alpha E + \beta E^2 + \gamma E^3 + \ldots$ rather than a Taylor series, values according to the former definition being a factor of six smaller than those obtained by the latter.
79 S.-J. Chung, S. Zheng, T. Odani, L. Beverina, J. Fu, L. A. Padilha, Arianna Biesso, J. M. Hales, X. Zhan, K. Schmidt, A. Ye, E. Zojer, S. Barlow, D. J. Hagan, E. W. Van Stryland, Y. Yi, Z. Shuai, A. GiorgioPagani, J.-L. Brédas, J. W. Perry and S. R. Marder, *J. Am. Chem. Soc.*, 2006, **128**, 14444.
80 The peak values are strongly dependent on the damping used and better agreement with experiment can be obtained by using a smaller damping. The value of 0.1 eV was used for consistency with the simulation of the 2PA spectrum shown in Fig. 6 in which this damping reproduces the vibrational broadening seen in the experimental 2PA spectrum.
81 An additional peak is seen in the calculated THG spectrum at much lower energy (corresponding to an experimental photon energy of *ca.* 0.50 eV) than experimentally investigated in ref. 26. The calculated dispersion is shown for a wider wavelength range in the ESI.
82 D. Deffieux, D. Bonafoux, M. Bordeau, C. Biran and J. Dunogues, *Organometallics*, 1996, **15**, 2041.
83 A. C. Spivey, D. J. Turner, M. L. Turner and S. Yeates, *Org. Lett.*, 2002, **4**, 1899.
84 Y. Lee and R. B. Silverman, *Tetrahedron*, 2001, **57**, 5339.
85 H. ElOuazzani, N. Khiar, I. Fernandez and F. Alcudia, *J. Org. Chem.*, 1997, **62**, 287.
86 We found that the intermediate 2-chloromethyl-4-*n*-hexylthiophene can also be obtained directly from the protected alcohol **11** using the same conditions used in ref. 9 for the preparation of this intermediate from **12**. However, this intermediate was formed less cleanly and attempted purification by column chromatography on silica gel resulted in decomposition.
87 G. M. Sheldrick, "*SHELXS-86, SHELXS-97, and SHELXL-97, Programs for Crystallography*", 1986 and 1997.
88 G. M. Sheldrick, "*SADABS v.2.03, Bruker / Siemens Area Detector Absorption Correction Program*", Madison, WI, USA, 2003.
89 J. D. Matichak, J. M. Hales, S. Ohira, S. Barlow, S.-H. Jang, A. K.-Y. Jen, J.-L. Brédas, J. W. Perry and S. R. Marder, *ChemPhysChem*, 2010, **11**, 130.
90 H.-C. Lin, H. Kim, S. Barlow, J. M. Hales, J. W. Perry and S. R. Marder, *Chem. Commun.*, 2011, **47**, 782.
91 A. D. Becke, *J. Chem. Phys.*, 1993, **98**, 5648.
92 R. G. Parr and W. Yang, "*Density-Functional Theory of Atoms and Molecules*", Oxford University Press, Oxford, 1989.
93 W. Koch and M. C. Holthausen, "*A Chemist's Guide to Density Functional Theory*", Wiley & Sons, New York, 2000.
94 While the configuration of **1** in a single crystal has been determined by X-ray crystallography, in solution a number of more-or-less iso-energetic configurations can be expected. The conformer chosen for the calculations is approximately described by i/ii/iii in Fig. 4a and is expected to be the least sterically hindered (see discussion of the crystal structure).
95 M. J. Frisch, G. W. Trucks, H. B. Schlegel, G. E. Scuseria, M. A. Robb, J. R. Cheeseman, J. A. Montgomery, T. Vreven, K. N. Kudin, J. C. Burant, J. M. Millam, S. S. Iyengar, J. Tomasi, V. Barone, B. Mennucci, M. Cossi, G. Scalmani, N. Rega, G. A. Petersson, H. Nakatsuji, M. Hada, M. Ehara, K. Toyota, R. Fukuda, J. Hasegawa, M. Ishida, T. Nakajima, Y. Honda, O. Kitao, H. Nakai, M. Klene, X. Li, J. E. Knox, H. P. Hratchian, J. B. Cross, C. Adamo, J. Jaramillo, R. Gomperts, R. E. Stratmann, O. Yazyev, A. J. Austin, R. Cammi, C. Pomelli, J. W. Ochterski, P. Y. Ayala, K. Morokuma, G. A. Voth, P. Salvador, J. J. Dannenberg, V. G. Zakrzewski, S. Dapprich, A. D. Daniels, M. C. Strain, O. Farkas, D. K. Malick, A. D. Rabuck, K. Raghavachari, J. B. Foresman, J. V. Ortiz, Q. Cui, A. G. Baboul, S. Clifford, J. Cioslowski, B. B. Stefanov, G. Liu, A. Liashenko, P. Piskorz, I. Komaromi, R. L. Martin, D. J. Fox, T. Keith, M. A. Al-Laham, C. Y. Peng, A. Nanayakkara, M. Challacombe, P. M. W. Gill, B. Johnson, W. Chen, M. W. Wong, C. Gonzalez, and J. A. Pople, "*Gaussian 03*", Wallingford, CT, 2004.
96 J. A. Pople, D. L. Beveridge and P. A. Dobosh, *J. Chem. Phys.*, 1967, **47**, 2026.
97 N. Mataga and K. Nishimoto, *Z. Phys. Chem.*, 1957, **13**, 140.
98 M. C. Zerner, G. H. Loew, R. F. Kichner and U. T. Mueller-Westerhoff, *J. Am. Chem. Soc.*, 1980, **102**, 589.
99 R. J. Buenker and S. D. Peyerimhoff, *Theor. Chim. Acta*, 1974, **35**, 33.
100 Z. Shuai, D. Beljonne and J.-L. Brédas, *J. Chem. Phys.*, 1992, **97**, 1132.
101 P. Tavan and K. J. Schulten, *Chem. Phys.*, 1986, **85**, 6602.
102 B. M. J. Pierce, *Chem. Phys.*, 1989, **91**, 791.
103 E. Zojer, D. Beljonne, T. Kogej, H. Vogel, S. R. Marder, J. W. Perry and J.-L. Brédas, *J. Chem. Phys.*, 2002, **116**, 3646 and references therein.
104 B. J. Orr and J. F. Ward, *Mol. Phys.*, 1971, **20**, 513.

